*Original Article*

Dose-Response:
An International Journal
January-March 2018:1-10

DOI: 10.1177/1559325817750068
journals.sagepub.com/home/dos
SAGE

# Homogenous and Microbeam X-Ray Radiation Induces Proteomic Changes in the Brains of Irradiated Rats and in the Brains of Nonirradiated Cage Mate Rats

**Richard Smith[1], Jiaxi Wang[2], Colin Seymour[1], Cristian Fernandez-Palomo[1], Jennifer Fazzari[1], Elisabeth Schültke[3], Elke Bräuer-Krisch[4], Jean Laissue[5], Christian Schroll[6], and Carmel Mothersill[1]**

## Abstract

To evaluate microbeam radiation therapy (MRT), for brain tumor treatment, the bystander effect in nonirradiated companion animals was investigated. Adult rats were irradiated with 35 or 350 Gy at the European Synchrotron Research Facility using homogenous irradiation (HR) or MRT to the right brain hemisphere. The irradiated rats were housed with nonirradiated rats. After 48 hours, all rats were euthanized and the frontal lobe proteome was analyzed using 2-dimensional electrophoresis and mass spectrometry. Proteome changes were determined by analysis of variance ($P < .05$). Homogenous irradiation increased serum albumin, heat shock protein 71 (HSP-71), triosephosphate isomerase (TPI), fructose bisphosphate aldolase (FBA), and prohibitin and decreased dihydrolipoyl dehydrogenase (DLD) and pyruvate kinase. Microbeam radiation therapy increased HSP-71, FBA, and prohibitin, and decreased aconitase, dihydropyrimidinase, TPI, tubulin DLD, and pyruvate kinase. Cage mates with HR irradiated rats showed increased HSP-71 and FBA and decreased pyruvate kinase, DLD, and aconitase. Cage mates with MRT irradiated rats showed increased HSP-71, prohibitin, and FBA and decreased aconitase and DLD. Homogenous irradiation proteome changes indicated tumorigenesis, while MRT proteome changes indicated an oxidative stress response. The bystander effect of proteome changes appeared antitumorigenic and inducing radioresistance. This investigation also supports the need for research into prohibitin interaction with HSP-70/71 chaperones and cancer therapy.

## Keywords

antitumorigenesis, bystander effect, homogenous irradiation, microbeam irradiation, proteomics

## Introduction

Microbeam radiation therapy (MRT) is an experimental radiotherapy concept characterized by the delivery of multiple, parallel and very narrow (~25-75 µm) microplanar X-ray beams.[1] The technique was initially investigated in the 1950s and there is now international effort to develop its clinical implementation.[2] Specifically, these doses are delivered in parallel beams, which focus the high dose along narrow microplanar tracks, thus sparing large volumes of interjacent normal tissue from radiation exposure.[3,4] Microbeam radiation therapy therefore allows the application of peak X-ray doses, which are greater than the doses usually used for cancer therapy, by 1 or 2 orders of magnitude (eg, 150-4000 Gy).[1] In theory, this offers a noninvasive means for treating brain tumors by delivering targeted radiation doses to precise locations within the brain (ie, the

[1] Department of Medical Physics and Applied Radiation Sciences, McMaster University, Hamilton, Ontario, Canada
[2] Mass Spectrometry Facility, Department of Chemistry, Queen's University, Kingston, Ontario, Canada
[3] Department of Radio-oncology, Rostock University Medical Centre, Rostock, Germany
[4] European Synchrotron Radiation Facility, Grenoble, France
[5] Institute of Pathology, University of Bern, Bern, Switzerland
[6] Stereotactic Neurosurgery and Laboratory for Molecular Neurosurgery, Freiburg University Medical Centre, Freiburg, Germany

Received 27 April 2017; received revised 07 July 2017; accepted 11 July 2017

**Corresponding Author:**
Richard Smith, Department of Animal Biosciences, University of Guelph, 50 Stone Road East, Guelph, Ontario, Canada N1G 2W1.
Email: rich.wilson.smith@gmail.com

exact site of the tumor) without significant functional damage to the brain tissue outside of the site of irradiation.[5]

Apart from the potential medical applications, MRT is also of particular interest to those studying the radiation-induced bystander effect (RIBE).[6,7] Radiation-induced bystander effect describes the response of nonirradiated cells which receive signals from irradiated cells.[8] Bystander effects have been documented in vitro[9] and in vivo, in animals as diverse as mice,[10] bullfrog tadpoles[11] and fish.[12] Thus, the bystander effect can extend the influence of radiation exposure beyond the cells or animal which received the radiation dose. Microbeam radiation therapy has been shown to induce a bystander effect in the nonirradiated hemisphere of an MRT irradiated rat brain[13,14] and also in the brains of completely nonirradiated "cage mate" rats, which had been housed with the MRT irradiated rats.[15]

The bystander effect has been induced following exposure to nontargeted whole-body radiation dose of less than 10 mGy.[5,16] Clearly, this is much less than the radiation doses used for MRT (see above). However, MRT by its nature does not involve radiation doses in the mGy range. Nevertheless, in terms of investigating the MRT-induced bystander effect, examining the effect caused by a lower MRT dose than would be employed for actual therapy is important. Thus, the present investigation used 35 and 350 Gy radiation doses. Three hundred fifty Gy falls within the range which is likely to be used for MRT (see above), whereas 35 Gy allows for a comparison of the bystander effect induced with an MRT dose by 1 order of magnitude less.

In addition, exposure to 35 and 350 Gy HR (ie, by an unsegmented beam) has been shown to result in proteomic changes in the rat brain which are indicative of potential tumorigenesis.[14] In contrast, the proteomic response, induced by the bystander effect in the nonirradiated hemisphere of rat brains exposed to 35 and 350 Gy MRT, indicated a potentially antitumorigenic response based on reactive oxygen species (ROS)-mediated apoptosis.[14]

There are no data on the proteomic changes resulting from an intermammalian bystander effect induced by MRT. However, in fish gills, the interanimal RIBE, induced by whole-body radiation, has also been found to result in a protective proteomic response.[17,18] Since the interanimal bystander effect could be important in our understanding of the clinical use of MRT, the objective of the present investigation was to extend the studies summarized above. Therefore, identical radiation doses were used,in the present investigation, to investigate this intermammalian bystander effect to those which were used to investigate the bystander effect in the nonirradiated hemisphere of an MRT irradiated rat brain. By analyzing the proteomic changes in the brain of HR and MRT irradiated rats and the nonirradiated cage mate rats, which were then housed with these irradiated rats for 48 hours, our aim was to extend our knowledge of the bystander effect in general and, specifically, the consequences of an intermammalian bystander effect when using MRT as a radiotherapeutic approach in the treatment of brain cancer.

## Materials and Methods

### *Rat Husbandry and Homogenous (HR) and Microbeam (MRT) Irradiation*

Rat (adult male, Wistar; 260-280 g), husbandry, radiation procedures, anesthesia and experimental ethical guidelines, and licensing have all been previously described.[14,15] Briefly, the rats were supplied by Charles River Laboratories (L'Abrelse, France) and held in the animal facility at the European Synchrotron Research Facility (ESRF), Grenoble, France, under European Union directive 2010/63/EU. All experimental procedures were carried out on anesthetized rats (as described elsewhere[14,15]) under guidelines issued by the French government and specifically covered by licenses 380325 and B3818510002 and approved by the International Evaluation Committee for Animal Welfare and Rights. A total of 45 rats were used in this investigation; 5 completely untreated rats taken directly from the ESRF animal facility, 4 rats exposed to a sham irradiation + 4 cage mates, 4 rats exposed to 35 Gy HR + 4 cage mates, 4 rats exposed to 350 Gy HR + 4 cage mates, 4 rats exposed to 35 Gy MRT + 4 cage mates, and 4 rats exposed to 350 Gy MRT + 4 cage mates.

The procedures for positioning the anesthetized rats on the goniometer and for homogenous field irradiation (HR), using a broad beam, and microbeam radiation (MRT), using a 100 × 14 mm high monochromatic anteroposterior beam, in the ESRF insertion device (ID) hutch 17 beamline, have also been previously described.[14,15] Microbeam radiation therapy irradiation was of the right hemisphere using an array composed of 50 quasi-parallel rectangular planar microbeams 25-μm thick with a 200 μm center-to-center distance. Homogenous irradiation entrance and MRT peak entrance radiation doses of 35 or 350 Gy were delivered and confirmed using Gafchromic films.[14,15]

In addition to completely untreated control rats, which never left the ESRF animal facility, a sham irradiation control was included in the study, the purpose being to determine whether proteomic responses occurred as a result of anesthesia and the handling and confinement associated with the HR and MRT irradiation. These sham irradiated rats were anesthetized and positioned in the ID hutch 17 in the same way and for the same period of time as the irradiated rats, but no radiation dose was administered.

### *Cage Mate Pairing, Tissue Collection, and Proteomic Analysis*

Following irradiation (or sham irradiation), the rats were transported back to the ESRF animal facility and placed in individual cages with a single marked, nonirradiated rat. After 48 hours, the rats were deeply anesthetized, beheaded, and dissected.[15] Brain tissue samples (5 mm × 5 mm × 3 mm) were taken from the center of the irradiation array in the right hemisphere of the irradiated rats and the matching area from sham irradiated rats, cage mate rats, and completely untreated control

rats. These samples were placed in aluminum foil and immediately frozen in liquid nitrogen and then stored at −80°C.

The brain samples from these rats were then analyzed using 2 dimensional (2-D) gel electrophoresis (2-DE). Thirty microgram samples of brain tissue were homogenized in 300-µL ice-cold 2-D lysis buffer; the buffer composition is detailed elsewhere.[19] The homogenate was clarified, by centrifugation (18 000*g* for 5 minutes at 4°C) and desalted, using commercially available Pierce desalt columns (Fisher Scientific, Markham, Ontario, Canada). Total protein concentration was then determined using a commercially available protein assay kit (Bio-Rad Laboratories Inc, Mississauga, Ontario, Canada) and 100 µg of total protein was subjected to 2-DE. All 2-DE was carried out using the Protean 2-DE system, first-dimension immobilized pH gradient (IPG) strips (pH 3-10), second-dimension gels (Bio-Rad Laboratories, Inc) and rehydration, and IPG equilibration and second-dimension running buffers (all purchased from Bio-Rad Laboratories, Inc). The full 2-DE protocol, including IPG rehydration, first dimension isoelectric focusing, second dimension Laemmli/12% acrylamide electrophoresis, gel fixing and staining with SYPRO-ruby stain (Bio-Rad Laboratories, Inc), and gel image capture, using a Fluor-S Max gel imager (Bio-Rad Laboratories, Inc), has been described elsewhere.[14]

Each tissue sample was run individually on a single gel. Any gels which were not of an acceptable quality for image analysis were completely rerun using a new 30-mg tissue sample from the rat brain. The gel images were then analyzed using Phoretix 2-D (V 2004) analytical software (Phoretix International, Newcastle, United Kingdom). It is important to stress this analysis was carried out as a blind study. The gels were given a random code number so that, during analysis, it was not known whether the gel was from an irradiated, sham irradiated, cage mate, or control rat. The gels were also calibrated for molecular size (*M*r) and isoelectric point (p*I*) using protein markers (Bio-Rad Laboratories, Inc) and the gel calibration facility of the Phoretix 2-D software.

## Two-Dimensional Gel Statistical Analysis

Once gel image analysis had been completed, the gel images were organized by treatment. Protein spots were then quantified by normalized volume, a parameter which combines spot size and intensity to give an index of expression. To fully illustrate any changes in protein expression, individual normalized spot volumes were divided by the mean normalized spot volume of the corresponding protein from untreated control rats to give a "fold-change" index of expression.[20] These fold changes were then compared using analysis of variance followed by least square difference analysis; a $P < .05$ was considered statistically significant. Consistent protein expression and the results of this statistical analysis were used to select protein spots for excision and identification. In other words, the protein spots selected for protein identification were those which were present on all the gels in the experiment and which showed a statistical difference in normalized volume when compared to the completely untreated control rats. By these criteria, 11 protein spots were selected (Figure 1). Note that no protein spots were found which were consistently absent (ie, downregulated to the point of nondetection) in any experimental treatment.

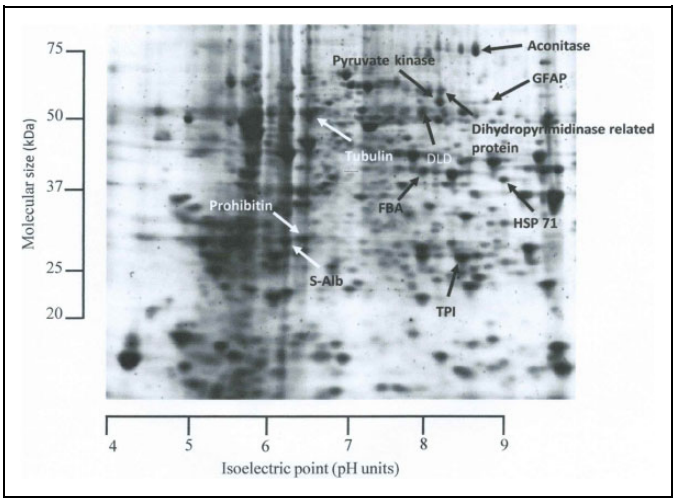


**Figure 1.** Representative 2-dimensional gel of a rat brain indicating the protein which were found to respond to direct homogenous radiation (HR) and microbeam radiation therapy (MRT) or in the brains of cage mate rats housed with those rats which received direct irradiation and also glial fibrillary acidic protein (GFAP); spot excised to confirm identification (refer to Discussion). (1) Aconitase, (2) dihydrolipoyl dehydrogenase (DLD), (3) dihydropyrimidinase, (4) fructose bisphosphate aldolase (FBA), (5) glial fibrillary acidic protein (GFAP), (6) heat shock protein 71 (HSP-71), (7) prohibitin, (8) pyruvate kinase, (9) serum albumin (S-Alb), (10) triosephosphate isomerase (TPI), and (11) tubulin.

## In-Gel Tryptic Digestion and Matrix-Assisted Laser Desorption Ionization QStar XL Mass Spectrometry Analysis

The full details of In-gel tryptic digestion and matrix-assisted laser desorption ionization (MALDI) mass spectrometry (MS) analysis have been described.[14] In summary, selected protein spots were excised, destained, reduced, treated with iodoacetamide, dehydrated, dried, and digested. The digested proteins were desalted and concentrated in formic acid and analyzed using a high-resolution QSTAR XL MALDI quadrupole time of flight (TOF) mass spectrometer (AB Sciex) coupled to a MALDI 2 ion source with a solid state Nd:YAG laser. Data acquisition was done by Analyst 1.1 Software (Applied Biosystems/MDS Sciex, Foster City, California, USA). Mass spectra in TOF MS and mass spectrometry/mass spectrometry (MS/MS) mode were in a mass range of 50 to 2500 m/z with a resolution of 8000 FWHM and a 60 V focusing potential was used throughout. The MS/MS data analysis was performed using MASCOT and peptide sequences were compared with the MS protein sequence database (MSDB). Tolerances for peptide information were 0.6 Da for MS and MS/MS, and all

**Table 1.** Results of Identification Analysis of the Proteins Indicated in Figure 1.

| Gel Spot[a] | Protein Description | MSDB Database Accession Code | Theor *Mr*[b] (kDa) | Theor p*I*[b] (pH units) | Exp *Mr*[c] (kDa) | Exp p*I*[c] (pH units) | MS/MS MOWSE Score[d] |
|---|---|---|---|---|---|---|---|
| 1 | Aconitase hydratase | ACON_MOUSE | 85.5 | 7.09 | 77.9 | 8.61 | 77 (28) |
| 2 | Dihydrolipoyl dehydrogenase | DLDH_MOUSE | 54.3 | 7.08 | 52.4 | 7.96 | 56 (38) |
| 3 | Dihydropyrimidinase-related protein | DPYL5_RAT | 61.5 | 6.27 | 59.1 | 8.22 | 58 (26) |
| 4 | Fructose-bisphosphate aldolase | ALDOC_HUMAN | 39.5 | 6.13 | 41.1 | 8.23 | 59 (44) |
| 5 | Glial fibrillary acidic protein | GFAP_CARAU | 42.6 | 4.85 | 53.4 | 8.66 | 58 (46) |
| 6 | Heat shock cognate 71 kDa protein | HSP7C_BOVIN | 71.2 | 5.25 | 38.4 | 8.88 | 59 (43) |
| 7 | Prohibitin | PHB_BOVIN | 29.8 | 5.43 | 30.0 | 6.59 | 106 (39) |
| 8 | Pyruvate kinase | KPYM_RAT | 57.8 | 6.30 | 55.2 | 8.34 | 52 (43) |
| 9 | Serum albumin | ALBU_BOVIN | 69.3 | 5.59 | 28.8 | 6.31 | 59 (39) |
| 10 | Triosephosphate isomerase | TPIS_BOVIN | 26.7 | 6.20 | 26.7 | 8.60 | 70 (40) |
| 11 | Tubulin alpha-1A | TBA1A_RAT | 50.1 | 4.84 | 50.1 | 6.70 | 52 (22) |

[a]The protein spots indicated in Figure 1.
[b]Theor, theoretically determined, that is, as listed on the MSDB database.
[c]Exp, experimentally determined, that is, as derived by 2-DE gel calibration.
[d]Figures in parenthesis indicate MOWSE score required for significant homology.

information was manually inspected based on *y* and/or *b* series ions (N-terminal carboxyl and bond-cleavage fragments from the C-terminal sides of the peptide, respectively).

## Results

### *Two-Dimensional Electrophoresis and Protein Identification*

Figure 1 illustrates a representative 2-D gel from the right hemisphere of a completely untreated control rat and indicates the protein spots selected for identification. Table 1 lists the protein identities as well as the theoretical (as listed by the protein database) and experimentally derived (determined by 2-D gel calibration) molecular sizes (*M*r; kDa) and isoelectric point (p*I*; pH units). A total of 11 protein spots showed consistent resolution on the gels across the entire experiment and statistically significant changes in expression (as defined by normalized spot volume).

The protein spots which were identified in this investigation as aconitase hydratase, dihydrolipoyl dehydrogenase (DLD), glial fibrillary acidic protein (GFAP), heat shock cognate 71 kDa (HSP-71), prohibitin, serum albumin (S-Alb), triosephosphate isomerase (TPI), and tubulin alpha-1A were the same identities as those derived from the corresponding protein spots in our previous investigation.[14] The spots identified as DLD, fructose bisphosphate aldolase (FBA), and pyruvate kinase were unique to this investigation. In our previous study,[14] we were not alerted to any change in the expression of these proteins.

The protein spots identified as DLD and prohibitin showed almost identical theoretical and experimentally derived *M*r and p*I* (Table 1). This suggests these were intact and unmodified molecules. The protein spots identified as aconitase hydratase, dihydropyrimidinase-related protein, FBA, pyruvate kinase, TPI, and tubulin alpha-1A also showed very similar theoretical and experimentally derived *M*r and p*I* (Table 1). Again this suggests these were intact molecules. However, the slightly different p*I* values suggest some modification. The experimentally derived *M*r of the protein spots identified as S-Alb and HSP-71 were less than the theoretical *M*r (Table 1), which suggests it is more likely these were breakdown products rather than intact molecules. It may therefore be more accurate to say that any changes in these proteins were more likely to be changes in protein turnover than changes in protein expression. The experimentally derived *M*r of GFAP was greater than the theoretical *M*r (Table 1). However, GFAP has been resolved at a similar *M*r, 45 to 55 kDa,[21] and an even greater *M*r, 68 kDa.[22] Again this suggests GFAP was most likely an intact molecule. Table 2 quantifies the changes to specific proteins in the right brain hemisphere of irradiated rats, as a result of HR or MRT, and in the right brain hemisphere of nonirradiated cage mate rats housed with the irradiated animals.

### *Proteomic Responses to Broad Beam Homogenous (HR) and Microbeam (MRT) Irradiation*

After 48 hours of HR, S-Alb, HSP-71, FBA, prohibitin, and TPI were found to increase in the right hemisphere of the rat brain. Serum albumin, HSP-71, and FBA were increased by 35 and 350 Gy, whereas prohibitin and TPI were unaffected by 35 Gy HR but were increased by 350 Gy. Two proteins were found to be reduced by HR after the same postirradiation interval: pyruvate kinase and DLD. Pyruvate kinase was decreased by 35 and 350 Gy HR, whereas DLD was unaffected by 35 Gy HR but decreased by 350 Gy HR.

Serum albumin was unaffected 48 hours after 35 or 350 Gy MRT but, as was the case with HR, HSP-71, FBA, and prohibitin were increased 48 hours after 35 and 350 Gy MRT. Microbeam radiation therapy also had a similar effect to HR on pyruvate kinase and DLD; 48 hours after irradiation with 35 or 350 Gy, pyruvate kinase was reduced, and 48 hours after irradiation with 350 Gy, MRT DLD was reduced. Tubulin,

**Table 2.** Fold Change (HR or MRT or Cage Mates to HR or MRT Normalized Spot Volume/Mean Handling Control Normalized Spot Volume) in the Expression of 11 Proteins Indicated in Figure 1.[a]

| | Direct Irradiation; Homogenous Radiation | | Direct Irradiation; Microbeam Radiation Therapy | | Cage Mates; Homogenous Radiation | | Cage Mates; Microbeam Radiation Therapy | |
|---|---|---|---|---|---|---|---|---|
| Protein | 35 Gy | 350 Gy | 35 Gy | 350 Gy | 35 Gy | 350 Gy | 35 Gy | 350 Gy |
| Aconitase | 0.8 (0.7/1.0) | 1.0 (0.8/1.1) | 0.6[b] (0.5/0.7) | 0.5[b] (0.3/0.7) | 0.6[b] (0.5/0.7) | 1.0 (0.8/1.3) | 0.9 (0.7/1.1) | 0.5[b] (0.3/0.7) |
| Dihydrolipoyl dehydrogenase | 1.0 (0.8/1.1) | 0.2[b] (0.2/0.3) | 0.9 (0.5/1.1) | 0.3[b] (0.2/0.5) | 0.5[b] (0.4/0.6) | 1.0 (0.5/1.4) | 1.0 (0.5/1.9) | 0.3[b] (0.1/0.8) |
| Dihydropyrimidinase | 0.9 (0.6/1.2) | 1.0 (0.6/1.1) | 0.9 (0.6/1.1) | 0.4[b] (0.2/0.6) | 1.0 (0.7/1.4) | 0.9 (0.8/1.2) | 0.9 (0.5/1.1) | 1.1 (1.1/1.2) |
| Fructose bisphosphate aldolase | 1.4[b] (1.3/1.4) | 1.3[b] (1.2/1.6) | 2.3[b] (2.2/2.5) | 1.3[b] (1.2/1.8) | 1.8[b] (1.4/2.1) | 1.7[b] (1.2/2.0) | 1.7[b] (1.3/2.2) | 2.5[b] (2.4/2.6) |
| Glial fibrillary acidic protein | 1.0 (0.6/1.4) | 1.0 (0.8/1.1) | 1.1 (0.9/1.3) | 1.0 (0.7/1.3) | 1.0 (0.7/1.5) | 1.2 (0.8/1.4) | 1.0 (0.8/1.5) | 0.9 (0.8/1.1) |
| Heat shock protein 71 | 2.1[b] (1.4/2.9) | 1.3[b] (1.2/1.7) | 2.5[b] (1.9/3.4) | 3.3[b] (1.7/4.3) | 4.4[b] (3.4/5.2) | 4.9[b] (4.4/5.7) | 4.1[b] (3.4/4.7) | 3.7[b] (1.8/6.4) |
| Prohibitin | 1.2 (0.9/1.5) | 2.1[b] (1.4/3.3) | 1.7[b] (1.5/1.9) | 1.6[b] (1.2/2.2) | 1.2 (0.7/1.4) | 1.2 (0.7/1.8) | 1.3 (0.9/1.6) | 1.9[b] (1.6/2.5) |
| Pyruvate kinase | 0.5[b] (0.3/0.7) | 0.3[b] (0.3/0.3) | 0.4[b] (0.2/0.6) | 0.2[b] (0.2/0.2) | 0.5[b] (0.3/0.9) | 0.3[b] (0.2/0.5) | 0.5[b] (0.3/0.9) | 0.5[b] (0.2/0.9) |
| Serum albumin | 2.5[b] (2.0/3.1) | 2.5[b] (1.8/3.1) | 1.0 (0.6/1.4) | 2.0[b] (1.6/2.5) | 1.3 (0.8/1.8) | 1.3 (0.5/2.0) | 1.0 (0.5/1.6) | 1.0 (0.5/1.7) |
| Triosephosphate isomerase | 0.8 (0.7/1.1) | 1.8[b] (1.4/2.1) | 0.7[b] (0.7/0.7) | 1.0 (0.7/1.1) | 1.0 (1.0/1.0) | 0.8 (0.7/1.1) | 0.9 (0.9/1.1) | 1.0 (0.9/1.0) |
| Tubulin | 0.9 (0.9/1.0) | 0.8 (0.7/1.1) | 0.2[b] (0.1/0.4) | 0.3[b] (0.3/0.5) | 0.9 (0.6/1.2) | 1.0 (0.6/1.2) | 1.0 (0.7/1.1) | 1.1 (0.8/1.3) |

Abbreviations: HR, homogenous irradiation; MRT, microbeam radiation therapy.
[a]Data shown as mean and, in parentheses, the min/max fold change (n = 5 handling control rats and n = 4 irradiated or cage mate rats).
[b]A significant change ($P < .05$) in protein expression compared with the control rats.

which was unaffected by HR, was also reduced by 35 and 350 Gy MRT. However, in direct contrast to 350 Gy HR, there was a reduction in TPI 48 hours after 35 Gy MRT. Aconitase and dihydropyrimidinase, which were also unaffected by HR, were both reduced 48 hours after exposure to 350 Gy MRT.

### *Homogenous Radiation: Cage Mate Responses*

Heat shock protein 71 and FBA were increased and pyruvate kinase was decreased in the brain of cage mate rats paired with rats exposed to either 35 Gy or 350 Gy HR. In other words, the cage mate rat changes in these proteins were identical to those seen in the irradiated rats. Dihydrolipoyl dehydrogenase in cage mate rats showed a decrease when paired with rats exposed to 35 Gy HR. Therefore, while not identical (DLD was reduced by both 35 and 350 Gy HR), the HR cage mate response was also similar to directly irradiated HR rats. TPI, serum albumin, and prohibitin, which showed increases in HR rats, were not affected in cage mate rats. Despite being unaffected by HR, aconitase was decreased in cage mates housed with rats exposed to 35 Gy HR.

### *Microbeam Radiation Therapy: Cage Mate Responses*

Heat shock protein 71 was increased in cage mate rats paired with rats exposed to 35 and 350 Gy MRT. Thus, HSP-71 was increased in all irradiated and all cage mate rats. Prohibitin was also increased in cage mate rats paired with rats exposed to 35 and 350 Gy MRT (ie, the same response as seen with MRT exposure). This cage mate response was unique to MRT; cage mates to HR rats showed no change in prohibitin. Fructose bisphosphate aldolase was increased in cage mates to 35 and 350 Gy MRT rats. This was the same response as seen in cage mates to 35 Gy and 350 Gy HR-exposed rats. However, only 35 Gy MRT resulted in increased FBA, so the increase seen in cage mates to 350 Gy MRT-exposed rats occurred despite there being no change in FBA in the irradiated animals.

Aconitase and DLD were downregulated in the brain of cage mate rats, after pairing with rats exposed to 350 Gy MRT. This was similar to the downregulation of aconitase in cage mates paired with rats exposed to 35 and 350 Gy HR and identical to the downregulation of DLD in cage mates paired with rats exposed to 350 Gy HR.

## Discussion

### *Methodology*

It should be recognized that tumor control involves the use of 2 MRT microbeam arrays which intersect orthogonally at the site of the tumor.[5,23-25] However, the investigation described here was intended as an extension of our previous study,[13] which involved MRT-induced bystander effects within the irradiated animal. Here, it was essential to ensure 1 hemisphere only was irradiated so that any proteomic changes in the completely nonirradiated hemisphere were due to a bystander effect. Therefore, a single MRT beam was used.[14] Since the objective of the present study was to compare bystander effect proteomic changes which occur within the irradiated rat with bystander effect proteomic changes induced in completely nonirradiated rats, we deliberately chose to use an identical radiation protocol, as well as an identical protein extraction method and 2-DE format. However, as stated before,[14] we concede that alternative protein extraction methods or narrower pH ranges may

reveal additional proteomic changes and the proteins reported here are not assumed to be an exhaustive list.

Sham irradiation was not found to affect any of the protein spots resolved on the gels of the sham irradiated or the cage mate rats which were paired with the sham irradiated rats. There were also no protein spots which were unique to, or absent from, the gels from sham irradiated rats or their cage mates. This suggests that anesthesia and the restraints necessary for irradiation did not exert a significant effect on the brain proteome.

## *Homogenous Radiation: Proteomic Evidence for Radiation Induced Cancer Progression*

The increase in S-Alb and TPI and the decrease in DLD in irradiated rats 48 hours after HR exposure were identical to the responses, which occurred between 4 and 12 hours after irradiation with the same 350 Gy HR doses.[14] Increased S-Alb albumin and TPI and decreased DLD have all been associated with tumor development or cancer progression.[14] The present investigation therefore supports the suggestion that focal high-dose HR (particularly 350 Gy) may induce tumorigenesis in the rat brain.[14]

The increase in prohibitin 48 hours after HR and MRT irradiation also showed considerable consistency to the increases in the same proteins at up to 12 hours after irradiation, with HR or MRT,[14] to 48 hours after irradiation. Therefore, the present investigation provides additional evidence that prohibitin is increased in the mammalian brain following irradiation. However, the association between prohibitin and cancer is less well defined.[14] As a result, the role of prohibitin in terms of causing cancer cell proliferation or suppression is regarded as controversial.[27]

The increase in FBA 48 hours after HR and MRT was not seen 4 to 12 hours after X-ray exposure,[14] which suggests that a 48-hour interval following irradiation was required to induce this change. In addition to X-ray exposure, FBA has been shown to be increased by gamma[26] and ultraviolet[28] radiation. However, like prohibitin, increased FBA is not always associated with cancer. An increase has been seen in colorectal cancer[29,30] and in a head and neck cancer cell line ($FaDu_{DD}$), under hypoxia,[31] but a decrease in FBA has been recorded in squamous cell carcinoma[32] and in HT-29 cells expressing the cancer stem cell marker CD133.[33]

## *Microbeam Radiation: Proteomic Evidence for Induced Oxidative Stress Response*

Previously, in the brain of MRT irradiated rats, the increase in S-Alb and TPI and the decrease in DLD, following HR, were also accompanied by the HR- and MRT-induced increase in aconitase, another well-documented indicator of tumorigenesis.[14] However, in the present investigation, there was no change in aconitase 48 hours after HR irradiation. Furthermore 48 hours after MRT, there was a reduction in aconitase expression. Collectively, these results suggest that the HR-induced effect on aconitase is limited to somewhere between 12 and 48 hours and that 48 hours after irradiation MRT had the opposite effect on aconitase to that seen between 4 and 12 hours after irradiation.

There is evidence that reducing aconitase activity is a factor in the metabolic rearrangement seen in cancer cells and, as a result, a reduction in expression may be an indicator or poor prognosis in gastric cancers.[34] However, there is little doubt that radiation in general[35,36] and radiotherapy in particular[37] result in oxidative stress. Aconitase itself is not only highly susceptible to oxidation,[38] but aconitase activity has also been shown to decrease, within 3 days after gamma radiation, specifically because of mitochondrial damage due to the action of ROS.[39] Dihydropyrimidinase and tubulin, proteins which were not found to show any change in expression between 4 and 12 hours after irradiation,[14] but which did show a decline in the present study, 48 hours after irradiation, are also known to be susceptible to oxidation damage and loss.[40,41] Moreover, 35 Gy MRT also resulted in a decline in TPI, that is, again the opposite effect to that caused by the same dose HR. Triosephosphate isomerase reduction is known to stimulate antioxidant metabolism and acts to prevent excessive ROS accumulation.[42] A decline in pyruvate kinase, as was consistently the result 48 hours after HR and MRT, irrespective of radiation dose, also results in the resistance to ROS, by inhibiting TPI via accumulation of phosphoenolpyruvate, that is, pyruvate kinase inhibition, via the resulting substrate accumulation, initiates a feedback mechanism which acts on TPI.[43] We therefore propose these results could be indicative of a radiation-induced oxidative stress response. Specifically, following MRT exposure, the decline in oxidation sensitive aconitase, dihydropyrimidinase, and tubulin combined with the counteracting antioxidant response of TPI and pyruvate kinase could be indicative of the "oxidative balance" which occurs between oxidative damage and antioxidant mechanisms.[44]

## *Bystander Effect-Induced Proteomics: Antitumorigenesis and Radioresistance*

The increase in HSP-71, in the brain of cage mate rats, was the only proteomic change in the present investigation which was similar to those induced by a bystander effect in the nonirradiated hemisphere of an MRT irradiated rat brain.[14] Perhaps most significantly the brains of cage mate rats did not include the proteomic changes previously associated with oxidative stress-mediated potentially antitumorigenic apoptosis; specifically, TPI, prohibitin, and tubulin did not show a decrease and GFAP did not show an increase.[14] Indeed, the increase in prohibitin, in the nonirradiated cage mate rat brain, was the opposite response to the decrease seen in the nonirradiated hemisphere of rats following cranial MRT irradiation.[14] It is also significant that the cage mate brain reductions in DLD, aconitase, and pyruvate kinase and the increase in FBA, while being identical to the reductions seen in irradiated rat brains, were not part of the bystander effect proteome changes in the nonirradiated hemisphere of rats following cranial MRT

irradiation.[14] Therefore, we conclude the present investigation provides proteomic evidence for a fundamental difference between the proteomic response in the brains of nonirradiated cage mate rats housed with irradiated rats and the proteomic response in the nonirradiated hemisphere of a rat brain irradiated by MRT.[14]

Despite the uncertainty between prohibitin expression and cancer progression (see above, Homogenous Radiation; Proteomic Evidence for Radiation Induced Cancer Progression), increased prohibitin expression can be the basis for tumor suppression.[45] Among its roles, prohibitin is a regulator of mitochondrial assembly.[46] One recent review has therefore highlighted the importance of prohibitin in preventing tumorigenesis, by stabilizing mitochondria and improving the efficacy of cancer treatment,[47] and 2 others have highlighted prohibitin mediated processes as targets for chemotherapy.[48,49] Specific examples of chemotherapeutic agents and increased prohibitin include platycodin[50] and etoposide.[51]

Apart from the reduction in prohibitin, the potential antitumorigenic consequences of a cage mate bystander effect is supported by the decrease in DLD. Dihydrolipoyl dehydrogenase expression increased in lymphoma cells,[52] which suggests that DLD downregulation in the cage mates would if anything be antitumorigenic. Interestingly, the same study[52] also mirrored the present investigation by showing a concomitantly higher expression of prohibitin in resting B cells compared with lymphoma cells.

In addition, one of the key proteomic responses in the brains or all nonirradiated rats which had been paired with HR or MRT irradiated rats was the increase in FBA. Fructose bisphosphate aldolase acts to improve cell function[53] by being part of an antioxidant protective response.[54,55] However, FBA is a target for oxidative stress.[56] An increase would therefore presumably compensate for any oxidative loss. Increased FBA is also a marker of increased radioresistance[57] or lower radiosensitivity.[28] Given that cage mate rats were not exposed to radiation, yet showed a similar increase in FBA to the HR and MRT irradiated rats, this common response adds further evidence to the conclusion that the bystander effect and induced radioresistance may not be due to the same mechanism.[58-60]

Proteomic evidence from the nonirradiated hemisphere of a rat brain irradiated by MRT strongly suggested a bystander effect which resulted in antitumorigenic response based on oxidative stress-induced apoptosis.[14] The proteomic data from the present investigation suggests a bystander effect in a nonirradiated rat brain, induced by the proximity of irradiated rats, is antitumorigenic, primarily via the stabilization of mitochondria, and may also confer a degree of radioresistance. Thus, despite differences in the actual proteins which show changes in expression, there may be some common aspects of the proteomic responses of the bystander effect induced in the nonirradiated hemisphere of an MRT irradiated rat brain and the bystander effect induced by an irradiated rat, in the brain of a completely nonirradiated animal.

The release of volatile secretions, as is the case in irradiated mice,[61] is one possible chemical signal vector which could induce these bystander effect proteomic changes. However work using fish, separated by a physical barrier, has also provided evidence for a physical component to the bystander signal.[62]

### *Bystander Effect Proteomics: HSP-71 and the Prevention of Neurological Degeneration*

One other finding from our previous study involving the bystander effect in the nonirradiated hemisphere of an MRT irradiated rat was the potential role of HSP-71 in ensuring that the antitumorigenic responses of GFAP, TPI, tubulin, and prohibitin are not negated by the same proteins being instrumental in neurodegeneration or the onset of neurological disorders, such as Alzheimer's or Huntington's disease or schizophrenia.[14] In the present investigation, changes in GFAP or TPI were not part of the cage mate/intermammalian proteomic response. However, FBA, an increase of which could be part of a protective/antitumorigenic response (see above), is both upregulated[63,64] and oxidized[65,66] in the brain of patients with Alzheimer disease. In addition, prohibitin is increased in the frontal cortex of patients with Parkinson disease.[67] Therefore a similar question exists, albeit involving different proteomic responses, to that raised by bystander effect proteomic changes in the nonirradiated hemisphere of an MRT irradiated rat brain,[14] as to whether the advantages of any potentially antitumorigenic proteomic changes could be negated by a detrimental effect on neurological function, also applies to the intermammalian bystander effect.

Heat shock protein 71 is the constitutively expressed member of the HSP-70 family.[68] Despite its inconsistency or contradictory association with cancer,[69] HSP-70/71 is (i) well documented as a chaperone, (ii) critical to ensuring the correct cellular response to neuronal stress tolerance, and (iii) protects against all of the neurological disorders listed above.[14] Heat shock protein 70 is also a positive predictor of survival following non-small cell lung cancer chemotherapy.[70] We therefore propose a similar integrative role for HSP-71 in the responses of the brain of a cage mate rat housed with an irradiated rat as we have for the nonirradiated hemisphere of an MRT irradiated rat brain.[14] We also propose that determining whether FBA and prohibitin act in a tumor suppressive and radioresistant capacity, in companion animals to those exposed to radiation, now warrants specific experimental attention.

## Conclusion

This investigation has demonstrated proteomic evidence for a RIBE in nonirradiated rats housed with rats exposed to HR or MRT. We propose these responses are potentially protective, specifically antitumorigenic, and possibly confer radioresistance. The increase in prohibitin was similar to the result of a bystander effect in the nonirradiated hemisphere of an MRT irradiated rat brain. This investigation therefore further supports the existing need for research into the role of prohibitin

in cancer therapy particularly with the interaction of HSP-70/71 chaperones.

## Acknowledgments

This experiment was performed on the ID17 beamline at the European Synchrotron Radiation Facility (ERSF), Grenoble, France, and we are grateful for the allocation of beam time and the assistance provided by the ID17 staff. We would also like to express our appreciation to Professor Lucy Lee, University of the Fraser River Valley, Abbotsford, British Columbia, Canada, for kindly allowing us to use her 2-D gel apparatus for this investigation.

## Declaration of Conflicting Interests

The author(s) declared no potential conflicts of interest with respect to the research, authorship, and/or publication of this article.

## Funding

The author(s) disclosed receipt of the following financial support for the research, authorship, and/or publication of this article: The COST Action TD1205 (SYRA3), The Canada Research Chairs Programme, The Natural Science and Engineering Research Council (NSERC), Discovery Grant Programme, and at the time of this investigation, Dr Schültke held a Marie Curie Reintegration Grant (PIRG07-GA-2010-268250).

## ORCID iD

Richard Smith http://orcid.org/0000-0002-8950-2386
Cristian Fernandez-Palomo http://orcid.org/0000-0002-5095-262X

## References

1. Bräuer-Krisch E, Serduc R, Siegbahn EA, et al. Effects of pulsed, spatially fractionated, microscopic synchrotron X-ray beams on normal and tumoral brain tissue. *Mutat Res*. 2010; 704(1-3): 160-166.
2. Bravin A, Olko P, Schültke E, Wilkens JJ. SYRA3 COST action—microbeam radiation therapy: roots and prospects. *Phys Med*. 2015;31(6):561-563.
3. Blattmann H, Gebbers JO, Bräuer-Krisch E, et al. Applications of synchrotron X-rays to radiotherapy. *Nucl Instrum Meth*. 2005; 548:17-22.
4. Grotzer MA, Schültke E, Bräuer-Krisch E, Laissue JA. Microbeam radiation therapy: clinical perspectives. *Phys Med*. 2015;31(6):564-567.
5. Schültke E, Juurlink BH, Ataelmannan K, et al. Memory and survival after microbeam radiation therapy. *Eur J Radiol*. 2008; 68(suppl 3):S142-S146.
6. Prise KM. New advances in radiation biology. *Occup Med (Lond)*. 2006;56(3):156-161.
7. Schettino G, Folkard M, Michael BD, Prise KM. Low-dose binary behavior of bystander cell killing after microbeam irradiation of a single cell with focused c(k) X rays. *Radiat Res*. 2005; 163(3): 332-336.
8. Mothersill C, Seymour C. Radiation-induced bystander effects—implications for cancer. *Nat Rev Cancer*. 2004;4(2):158-164.
9. Morgan WF. Non-targeted and delayed effects of exposure to ionizing radiation: I. radiation-induced genomic instability and bystander effect in vitro. A review. *Radiat Res*. 2003;159(5): 567-580.
10. Isaeva VG, Surinov BP. Postirradiation volatile secretion and development on immunosuppression effects by laboratory mice with various genotype. *Radiats Biol Radioecol*. 2007;47(1): 10-16.
11. Audette-Stewart M, Yankovich T. Bystander effects in bullfrog tadpoles. *Radioprotection*. 2011;46(6):S497-S497.
12. Mothersill C, Bucking C, Smith RW, et al. Communication of radiation-induced bystander signals between fish in vivo. *Environ Sci Technol*. 2006;40(21):6859-6864.
13. Fernandez-Palomo C, Schültke E, Smith R, et al. Bystander effect in tumor-free and tumor-bearing rat brains following irradiation by synchrotron X-rays. *Int J Radiat Biol*. 2013;89(6):445-453.
14. Smith RW, Wang J, Schültke E, et al. Proteomic changes in the rat brain induced by homogenous irradiation and by the bystander effect resulting from high energy synchrotron X-ray microbeams. *Int J Radiat Biol*. 2013;89(2):118-127.
15. Mothersill C, Fernandez-Palomo C, Fazzari J, et al. Transmission of signals from rats receiving high doses of microbeam radiation to cage mates: an inter-mammal bystander effect. *Dose Response*. 2014;12(1):72-92.
16. Liu Z, Mothersill C, McNeill F, et al. A dose threshold for a medium transfer bystander effect for a human skin cell line. *Radiat Res*. 2006;163(1 pt 1):19-23.
17. Smith RW, Wang J, Bucking CP, Mothersill CE, Seymour CB. Evidence for a protective response by the gill proteome of rainbow trout exposed to X-ray induced bystander signals. *Proteomics*. 2007;7(22):4171-4180.
18. Smith RW, Wang J, Mothersill CE, Hinton TG, Aizawa K, Seymour CB. Proteomic changes in the gills of wild-type and transgenic radiosensitive medaka following exposure to direct irradiation and to X-ray induced bystander signals. *Biochim Biophys Acta*. 2011;1814(2):290-298.
19. Smith RW, Wood CM, Cash P, et al. Apolipoprotein AI could be a significant determinant of epithelial integrity in rainbow trout gill cell cultures: a study in functional proteomics. *Biochim Biophys Acta*. 2005;1749(1):81-93.
20. Lim YB, Pyun BJ, Lee HJ, Jeon SR, Jin YB, Lee YS. Proteomic identification of radiation responses markers in mouse intestine and brain. *Proteomics*. 2011;11(7):1254-1263.
21. Aksenov MY, Aksenova MV, Butterfield DA, Geddes JW, Markesbery WR. Protein oxidation in the brain in Alzheimer's disease. *Neuroscience*. 2001;103(2):373-383.
22. Choi J, Forester MJ, McDonald SR, et al. Proteomic identification of specific oxidized proteins in ApoE-knockout mice: relevance to Alzheimer's disease. *Free Radic Biol Med*. 2004;36(9): 1155-1162.
23. Bouchet A, Bräuer-Krisch E, Prezado Y, et al. Better efficacy of synchrotron spatially microfractionated radiation therapy than uniform radiation therapy on glioma. *Int J Radiat Oncol Biol Phys*. 2016;95(5):1485-1494.
24. Laissue JA, Geiser G, Spanne PO, et al. Neuropathology of ablation of rat gliosarcomas and contiguous brain tissues using a microplanar beam of synchrotron-wiggler-generated X rays. *Int J Cancer*. 1998;78(5):654-660.

25. Serduc R, Bouchet A, Bräuer-Krisch E, et al. Synchrotron microbeam radiation therapy for rat brain tumor palliation-influence of the microbeam width at constant valley dose. *Phys Med Biol*. 2009;54(21):6711-6724.
26. Theiss AL, Sitaraman SV. The role and therapeutic potential of prohibitin 520 in disease. *Biochim Biophys Acta*. 2011;1813(6): 1137-1143.
27. Sriharshan A, Bold K, Sarioglu H, et al. Proteomic analysis by SILAC and 2D-DIGE reveals radiation-induced endothelial response: four key pathways. *J Proteomics*. 2012;75(8): 2319-2330.
28. Lu J, Suzuki T, Satoh M, et al. Involvement of aldolase A in X-ray resistance of human HeLa and $UV^r$-1 cells. *Biochem Biophys Res Commun*. 2008;369(3):948-952.
29. Đermadi Bebek D, Valo S, Pussila M, et al. Inherited cancer predisposition sensitizes colonic mucosa to address western diet effects and putative cancer-predisposing changes on mouse proteome. *J Nutr Biochem*. 2014;25(11):1196-1206.
30. Muto T, Taniguchi H, Kushima R, et al. Global expression study in colorectal cancer on proteins with alkaline isoelectric point by two-dimensional difference gel electrophoresis. *J Proteomics*. 2011;74(6):858-873.
31. Singers Sørensen B, Horsman MR, Vorum H, et al. Proteins upregulated by mild and severe hypoxia in squamous cell carcinomas in vitro identified by proteomics. *Radiother Oncol*. 2009; 92(3):443-449.
32. Qi YJ, Chao WX, Chiu JF. An overview of esophageal squamous cell carcinoma proteomics. *J Proteomics*. 2012;75(11): 3219-3137.
33. Lee HN, Park SH, Lee EK, Bernardo R, Kim CW. Proteomic profiling of tumor-initiating cells in HT-29 human colorectal cancer cells. *Biochem Biophys Res Commun*. 2012;427(1): 171-177.
34. Desideri E, Vegliante R, Ciriolo MR. Mitochondrial dysfunctions in cancer: genetic defects and oncogenic signaling impinging on TCA cycle activity. *Cancer Lett*. 2015:356(2 pt A):217-223.
35. Huang TT, Zou Y, Corniola R. Oxidative stress and adult neurogenesis—effects of radiation and superoxide dismutase deficiency. *Semin Cell Dev Biol*. 2012;23(7):738-744.
36. Zhang Y, Martin SG. Redox proteins and radiotherapy. *Clin Oncol (R Coll Radiol)*. 2014;26(5):289-300.
37. Ozben T. Oxidative stress and apoptosis: impact on cancer therapy. *J Pharm Sci*. 2007;96(9):2181-2196.
38. Mangialasche F, Polidori MC, Monastero R, et al. Biomarkers of oxidative and nitrosative damage in Alzheimer's disease and mild cognitive impairment. *Ageing Res Rev*. 2009;8(4):285-305.
39. Chung HC, Kim SH, Lee MG, et al. Mitochondrial dysfunction by gamma irradiation accompanies the induction of cytochrome P450 2E1 (CYP2E1) in rat liver. *Toxicology*. 2001;161(1-2):79-91.
40. Butterfield DA, Abdul HM, Newman S, Reed T. Redox proteomics in some age-related neurodegenerative disorders or models thereof. *NeuroRx*. 2006;3(3):344-357.
41. Allani PK, Sum T, Bhansali SG, Mukherjee SK, Sonee M. Comparative study of the effect of oxidative stress on the cytoskeleton in human cortical neurons. *Toxicol Appl Pharmacol*. 2004;196(1): 29-36.
42. Ring J, Sommer C, Carmona-Gutierrez D, Ruckenstuhl C, Eisenberg T, Madeo F. The metabolism beyond programmed cell death in yeast. *Exp Cell Res*. 2012;318(11):1193-1200.
43. Grüning NM, Rinnerthaler M, Bluemlein K, et al. Pyruvate kinase triggers a metabolic feedback loop that controls redox metabolism in respiring cells. *Cell Metab*. 2011;14(3):415-427.
44. Einor D, Bonisoli-Alquati A, Costantini D, Mousseau TA, Møller AP. Ionizing radiation, antioxidant response and oxidative damage: a meta-analysis. *Sci Total Environ*. 2016;548-549:463-471.
45. Bulteau AL, Bayot A. Mitochondrial proteases and cancer. *Biochim Biophys Acta*. 2011;1807(6):595-601.
46. Maceyka M, Harikumar KB, Milstien S, Spiegel S. Sphingosine-1-phosphate signalling and its role in disease. *Trends in Cell Biol*. 2012;22(1):50-60.
47. Koushyar S, Jiang WG, Dart DA. Unveiling the potential of prohibitin in cancer. *Cancer Lett*. 2015;369(2):316-322.
48. Thuaud F, Ribeiro N, Nebigi CG, Désaubry L. Prohibitin ligands in cell death and survival: mode of action and therapeutic potential. *Chem Biol*. 2013;20(3):316-331.
49. Asati V, Mahapatra DK, Bharti SK. PI3K/Akt/mTOR and Ras/Raf/MEK/ERK signalling pathways inhibitors as anticancer agents: structural and pharmacological perspectives. *Eur J Med Chem*. 2016;109:314-341.
50. Lu JJ, Lu DZ, Chen YF, et al. Proteomic analysis of hepatocellular carcinoma HepG2 cells treated with platycodin D. *Chin J Nat Med*. 2015;13(9):673-0679.
51. Paul D, Chanukuppa V, Reddy PJ, et al. Global proteomic profiling identifies etoposide chemoresistance markers in non-small cell lung carcinoma. *J Proteomics*. 2016;138:95-105.
52. Romesser PB, Perlman DH, Faller DV, Costello CE, McComb ME, Denis GV. Development of a malignancy-associated proteomic signature for diffuse large B-cell lymphoma. *Am J Pathol*. 2009;175(1):25-35.
53. Marques-Aleixo I, Oliveira PJ, Moreira PI, Ascensão A. Physical exercise as a possible strategy for brain protection: evidence from mitochondrial-mediated mechanisms. *Prog Neurobiol*. 2012; 99(2):149-162.
54. Opii WO, Joshi G, Head E, et al. Proteomic identification of brain proteins in the canine model of human aging following a long-term treatment with antioxidants and a program of behavioral enrichment: relevance to Alzheimer's disease. *Neurobiol Aging*. 2008;29(1):51-70.
55. Perluigi M, Swomley AM, Butterfield DA. Redox proteomics and the dynamic molecular landscape of the aging brain. *Ageing Res Rev*. 2014;13:75-89.
56. Aguilar-Melero P, Ferrín G, Muntané J. Effects of nitric oxide synthase-3 overexpression on posttranslational modifications and cell survival in HepG2 cells. *J Proteomics*. 2012;75(3): 740-755.
57. Smith L, Qutob O, Watson MB, et al. Proteomic identification of putative biomarkers of radiotherapy resistance: a possible role for the 26S proteasome? *Neoplasia*. 2009;11(11):1194-1207.
58. Mothersill C, Seymour CB, Joiner MC. Relationship between radiation-induced low-dose hypersensitivity and the bystander effect. *Radiat Res*. 2002;157(5):526-532.

59. Ryan LA, Seymour CB, Mothersill CE. Investigation into non-linear adaptive responses and split dose recovery induced by ionizing radiation in three human epithelial derived cell lines. *Dose Response*. 2009;7(4):292-306.
60. Smith RW, Mothersill C, Hinton T, et al. Exposure to low level chronic radiation leads to adaptation to a subsequent acute X-ray dose and communication of modified acute X-ray induced bystander signals in medaka (Japanese rice fish, *Oryzias latipes*). *Int J Radiat Biol*. 2011;87(10):1011-1022.
61. Surinov BP, Isaeva VG, Dukhova NN. Postirradiation volatile secretions of mice: syngeneic and allogeneic immune and behavioural effects. *Bull Exp Biol Med*. 2004;138(4):384-386.
62. Mothersill C, Smith RW, Fazzari J, McNeill F, Prestwich W, Seymour CB. Evidence for a physical component to the radiation-induced bystander effect. *Int J Rad Biol*. 2012;88(8): 583-591.
63. Aluise CD, Sowell Robinson RA, Beckett TL, et al. Preclinical Alzheimer disease: brain oxidative stress, Aβ peptide and proteomics. *Neurobiol Dis*. 2010;39(2):221-228.
64. Kang MG, Byun K, Kim JH, et al. Proteogenomics of the human hippocampus: the road ahead. *Biochim Biophys Acta*. 2015; 1854(7):788-797.
65. Butterfield DA, Di Domenico F, Barone E. Elevated risk of type 2 diabetes for development of Alzheimer disease: a key role for oxidative stress in brain. *Biochim Biophys Acta*. 2014;1842(9): 1693-1706.
66. Chang RYK, Etheridge N, Dodd PR, Nouwens AS. Targeted quantitative analysis of synaptic proteins in Alzheimer's disease brain. *Neurochem Int*. 2014;75:66-75.
67. Ferrer I, Perez E, Dalfó E, Barrachina M. Abnormal levels of prohibitin and ATP synthase in the substantia nigra and frontal cortex in Parkinson's disease. *Neurosci Lett*. 2007;415(3):205-209.
68. Hatayama T, Fujio N, Yukioda M, Funae Y, Kinoshita H. Separation of rat liver HSP70 and HSP71 by high-performance liquid chromatography with a hydroxylapatite column. *J Chromatogr*. 1989;481:403-410.
69. Kurahashi T, Miyake H, Hara I, Fujisawa M. Expression of major heat shock proteins in prostate cancer: correlation with clinicopathological outcomes in patients undergoing radical prostatectomy. *J Urol*. 2007;177(2):757-761.
70. Park TS, Kim H-R, Koh JS, et al. Heat shock protein 70 as a predictive marker for platinum-based adjuvant chemotherapy in patients with resected non-small cell lung cancer. *Lung Cancer*. 2014;86(2):262-267.